OPEN ACCESS
Saudi Journal of Engineering and Technology
Abbreviated Key Title: Saudi J Eng Technol
ISSN 2415-6272 (Print) | ISSN 2415-6264 (Online)
Scholars Middle East Publishers, Dubai, United Arab Emirates
Journal homepage: https://saudijournals.com

Original Research Article

Measurements of Stray Radiation from Medical Devices in Hospitals

Samir A Hamouda[1*], Marwa Abdelmaged Al-Howty[2]

[1]Department of Physics, University of Benghazi, Libya
[2]Benghazi Medical Center

DOI: https://doi.org/10.36348/sjet.2024.v09i10.001 | **Received:** 23.07.2024 | **Accepted:** 04.09.2024 | **Published:** 23.10.2024

***Corresponding author:** Samir A Hamouda
Department of Physics, University of Benghazi, Libya

Abstract

The main objective of this study was to look for the electromagnetic interference produced by medical devices in hospitals and to evaluate its impacts on the proper functions of such devices. However, the present study encountered other important problems with regard to CT scanner and X-ray Imaging systems. Such problems demand fast responses in order to secure health safety for the patients and the operators of such systems.

Keywords: Imaging Devices, CT scanner, X-Ray Imaging, Shielding, Electromagnetic Radiation, Medical Devices.

INTRODUCTION

The impacts of electromagnetic interference on electrical and electronics have been introduced elsewhere [1]. Radiation consists of electric and magnetic fields. It comes from natural and human resources. Artificial resources are used to generate high-level electromagnetic radiation, which may be commonly found in medical devices such as magnetic resonance imaging (MRI), computed tomography (CT), and X-rays [2]. The human body has the ability to absorb X-rays, which may be harmful and can cause various diseases such as cancer, mental disorders, neurological diseases, fetal malformations, cardiovascular diseases [2]. This is due to the severe damage they cause to the chemical bonds between living tissues. Long-term exposure to X-rays can also change the genetic characteristics of the organism and cause variations that lead to cancer. Exposure to high-radiation energy such as X-rays, gamma rays, and ultraviolet rays through the use of modern imaging techniques is a source of serious biological changes and harmful effects on the organism [2]. Recent studies have shown that exposure to dental X-rays may be associated with an increased risk of thyroid cancer [3]. This study shows the necessity of examining the imaging devices in hospitals in order to know the health safety of these devices for the patient and the operator, and to determine the aspects of effectiveness and weakness in shielding these devices and the extent of the safety of operation for workers.

METHODS AND MATERIALS

Figure 1, Shows the main units of the CT scanner. It can be seen fromfigure1. that the main units consist of X-ray tubes, Photon detectors, filters, collimator, shielding elements, the patient table, the image processor and the console (control unit). The function of each unit can be found in [4].

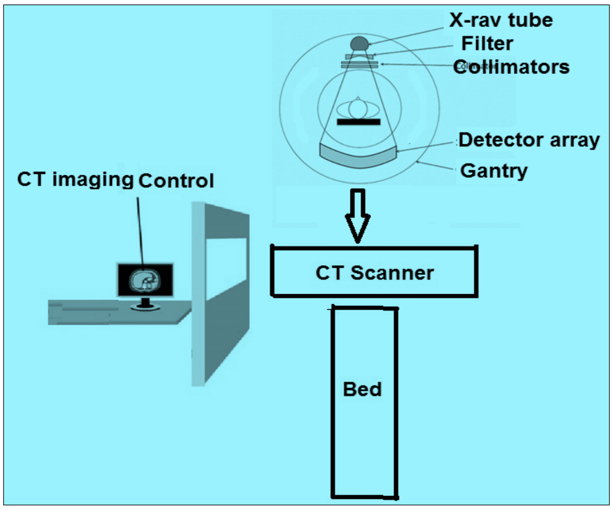

Figure 1: The CT scanner system with its main units

The energy stored in electromagnetic field consists of two parts: One part deals with the electric component (E) and the other part deals with the magnetic component (B). The energy stored in the electric component (E_e) is calculated as [5, 6]:

$$E_e = \frac{1}{2} \varepsilon_0 E^2 \quad (1)$$

Where E is the maximum amplitude of the magnetic field and ε_0 is the permittivity of free space. The energy stored in the magnetic component (E_m) is given as [5, 6]:

$$E_m = \frac{1}{2\mu_0} B^2 \quad (2)$$

Where B is the maximum amplitude of the magnetic field and μ_0 is the permeability of free space. The total energy stored in the electromagnetic radiation (E_{total}) is the sum of E_e and B_m

$$E_{total} = \frac{1}{2} \varepsilon_0 E^2 + \frac{1}{2\mu_0} B^2 \quad (3)$$

The X-ray source of the CT scanner is characterized in table 1**,** as follows:

Table1: x-ray tube operating conditions

x-ray tube	(tungsten)
x-ray tube current	400 mA
x-ray tube voltage	140 KV
x-ray tube capacity	5 MHU

The emission spectrum from Tungsten target (W) is shown in figure 2. The emission spectrum is consisted of two parts, the continuous spectrum (Bremsstrahlung radiation) and the characteristic lines. The energies of the characteristic lines were summarized in figure 2.

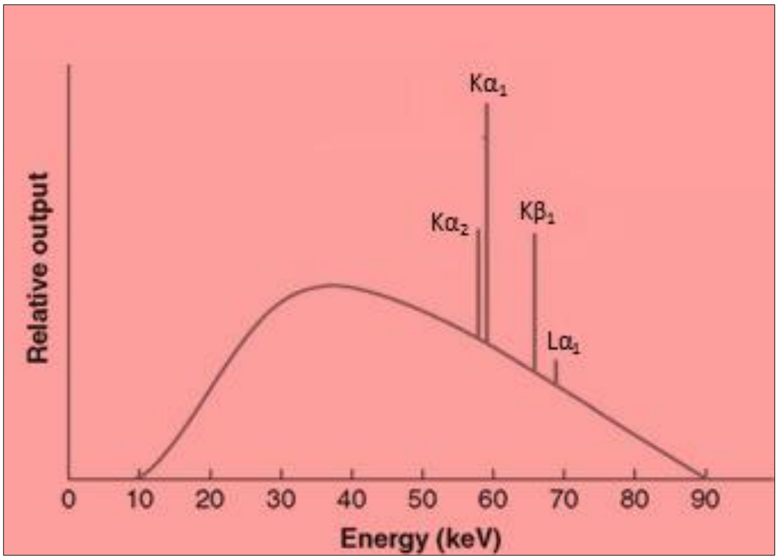

Figure 2: The emission spectrum of tungsten X-ray tube [7]

Table2**.** Shows the characteristic line energies for tungsten X-ray tube.

Table 2: The characteristic lines of tungsten target

Characteristic lines	$K\alpha_1$	$K\alpha_2$	$K\beta_1$	$L\alpha_1$	$L\alpha_2$	Lβ1	$L\beta_2$	$L\gamma_1$
Energy (KeV)	59.31	57.98	67.24	8.39	8.33	9.67	9.96	11.28

It can be seen from table 2, that the main emission line of tungsten tube is $K\alpha_1$ which has energy of 59.31KeV. This characteristic line has the highest emission of photons with energy 59.31KeV and is the principle line used in CT scanners.

The number of counts per second (N/s) was calculated using this formula:

$$N/s = \frac{E_{total}}{59.31 KeV}$$

The device used for measurements of electric (E) and magnetic (B) components of the electromagnetic radiation were of type Soeks Impulse Electromagnetic Field (EMF) Indicator. Figure 3, shows an image of such a system.

Figure 3: Measuring device used for this study

"Impulse" is made for the detection and localization of dangerous electromagnetic field zones. Soeks Impulse Specification is given in table 3.

Table 3: Specification of Soeks Impulse used for measurements

Device version	NUC-078 V4
Measurable electromagnetic field frequency range, Hz	from 20 to 2,000
Measurement range of electric field intensity amplitude along X, Y, Z axes, V/m	from 10 to 1,000
Measurement range of magnetic field (uT)	from 0.08 to 20
3 sensors of magnetic field 2 sensors of the electric field	every sensor makes a measurement in its axis

Primary measurements from the CT scanner have indicated that there was a stray radiation. Stray radiation implies that there were leakage and scatter radiation emanating from the source assembly and radiation produced even when the source assembly was at standby mode.

Measurements of stray radiation from CT scanner were carried out in three stages: one stage when the system at calibration mode. The second stage when the system at operation mode and the third stage when the system at standby mode. All these measurements were taken at the operator position (at nearby control room) which was about 4m from the CT assembly

RESULTS AND DISCUSSION: Table4**,** shows data collection when the CT scanner assembly at calibration mode.

Table 4: Data collected when the CT system at calibration mode

Meas.	E(V/m)	B (T)	E_{total} (J)	N/s	f (Hz)
1	510	$1.32x10^{-6}$	$1.8448x10^{-7}$	$1.8x10^{8}$	$3.4x10^{19}$ Hz
2	590	$1.69x10^{-6}$	$2.6775x10^{-7}$	$2.8x10^{8}$	$3.4x10^{19}$ Hz
3	840	$2.41x10^{-6}$	$5.435x10^{-7}$	$5.7x10^{8}$	$3.4x10^{19}$ Hz
4	1050	$2.80x10^{-6}$	$8.012x10^{-7}$	$8.4x10^{8}$	$3.4x10^{19}$ Hz
5	1230	$3.67x10^{-6}$	$1.2057x10^{-6}$	$1.3x10^{9}$	$3.4x10^{19}$ Hz
6	1390	$3.95x10^{-6}$	$1.4762x10^{-6}$	$1.6x10^{9}$	$3.4x10^{19}$ Hz
7	1580	$4.36x10^{-6}$	$1.8615x10^{-6}$	$1.96x10^{9}$	$3.4x10^{19}$ Hz
8	1400	$3.68x10^{-6}$	$1.4065x10^{-6}$	$1.5x10^{9}$	$3.4x10^{19}$ Hz
9	1160	$2.92x10^{-6}$	$9.352x10^{-7}$	$9.8x10^{8}$	$3.4x10^{19}$ Hz

Table 5, Presents data collection when the CT scanner assembly at operation mode.

Table 5: Measurements of electric and magnetic components of radiation when the CT scanner assembly at operation mode

Meas.	E(V/m)	B (T)	E_{total} (J)	N/s	f (Hz)
1	1030	$4.17x10^{-6}$	$1.1616x10^{-6}$	$1.2x10^{9}$	$3.4x10^{19}$ Hz
2	720	$3.27x10^{-6}$	$6.55x10^{-7}$	$6.9x10^{8}$	$3.4x10^{19}$ Hz
3	510	$1.73x10^{-6}$	$2.3423x10^{-7}$	$2.47x10^{8}$	$3.4x10^{19}$ Hz
4	680	$2.02x10^{-6}$	$3.6706x10^{-7}$	$3.87x10^{8}$	$3.4x10^{19}$ Hz
5	700	$1.70x10^{-6}$	$3.319x10^{-7}$	$3.5x10^{8}$	$3.4x10^{19}$ Hz
6	740	$1.83x10^{-6}$	$3.757x10^{-7}$	$3.96x10^{8}$	$3.4x10^{19}$ Hz
7	340	$0.76x10^{-6}$	$7.416x10^{-8}$	$7.82x10^{7}$	$3.4x10^{19}$ Hz
8	920	$2.47x10^{-6}$	$6.175x10^{-7}$	$6.51x10^{8}$	$3.4x10^{19}$ Hz
9	700	$2.07x10^{-6}$	$3.874x10^{-7}$	$4.1x10^{8}$	$3.4x10^{19}$ Hz
10	270	$1.20x10^{-6}$	$1.77x10^{-7}$	$1.86x10^{8}$	$3.4x10^{19}$ Hz

Table6, shows data collection when the CT scanner assembly at standby mode.

Table 6: Measurements of electric and magnetic components of radiation when the CT scanner assembly at standby mode

Meas.	E(V/m)	B(T)	E_{total} (J)	N/s	f (Hz)
1	300	$0.82x10^{-6}$	$6.66x10^{-8}$	$7.02x10^{7}$	$3.4x10^{19}$ Hz
2	300	$1.18x10^{-6}$	$9.525x10^{-8}$	$1.0x10^{8}$	$3.4x10^{19}$ Hz
3	360	$0.76x10^{-6}$	$8.03x10^{-8}$	$8.47x10^{7}$	$3.4x10^{19}$ Hz
4	450	$1.02x10^{-6}$	$1.3104x10^{-7}$	$1.38x10^{8}$	$3.4x10^{19}$ Hz
5	450	$0.80x10^{-6}$	$1.1511x10^{-7}$	$1.2x10^{8}$	$3.4x10^{19}$ Hz
6	360	$0.66x10^{-6}$	$7.47x10^{-8}$	$7.8x10^{7}$	$3.4x10^{19}$ Hz

Figure 4, summarize the results of measurements for the three stages

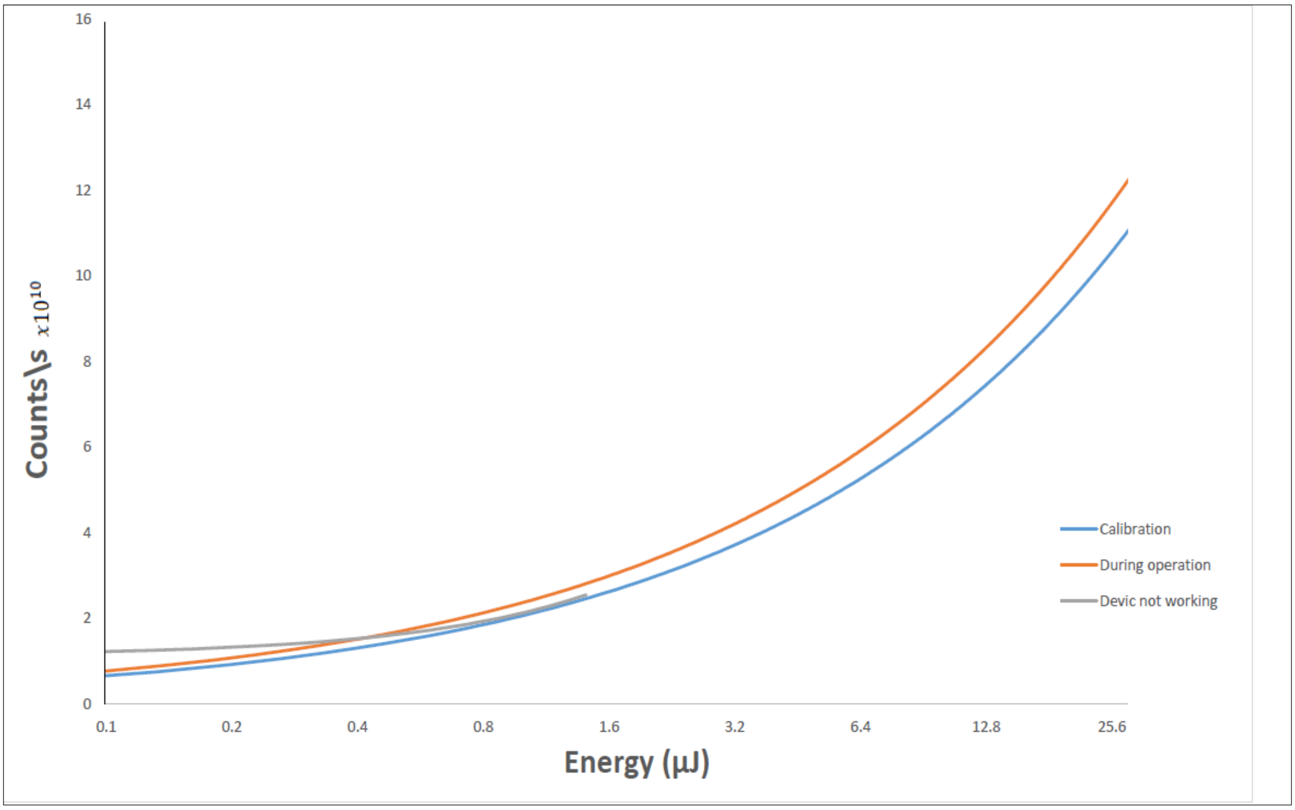

Figure 4: the results of measurements for the CT scanner at calibration, during operation and standby modes

It can be stated that the results presented in figure4, have shown that there is some kind of X-ray leakage, and this may be due to two reasons: The first reason is the stray radiation (random radiation) from the source and the second reason may be due to the radiation beam.

The shape of the curve shows that the radiation intensity starts at a low level and gradually increases with time. This is due to the source rotating 360 degrees, which in turn moves the source away from a specific point, which is the operator, and approaches it when it completes a full rotation.

Of course, this curve reflects the radiation transmitted from the CT and the number of ionizing photons per second relative to the characteristic k_α line. Hence, it is necessary to mention and focus on its importance, as these measurements were made in the control room, specifically at the operator's location which was at a distance of 2.40m from the center of the CT system.

These measurements have showed that the operator is exposed to high doses of ionizing radiation with energy ranging from 59.13-240keV, daily at a rate of 10 cases, each case takes about 15 minutes, i.e. at a rate of two and a half hours daily.

It can also be said that the measuring device sometimes becomes blind to the intensity of the radiation leaking at the operator's location. We conclude from these measurements that the CT system has no effective biological shielding materials. The lack of proper shielding material for the CT scanner system will have severe health consequences on the operator and other personal in the control room.

Figure 5 shows the correlation between electric field E and magnetic field B in the electromagnetic radiation.

Since there is a wide range of radiation energy emitted from the tungsten target of x-ray tube (~ 59-240 keV), the emerging points are as the electric field increases the magnetic field increases as well. The total energy of the electromagnetic radiation is shared by half due to electric field and the other half is due to magnetic field.

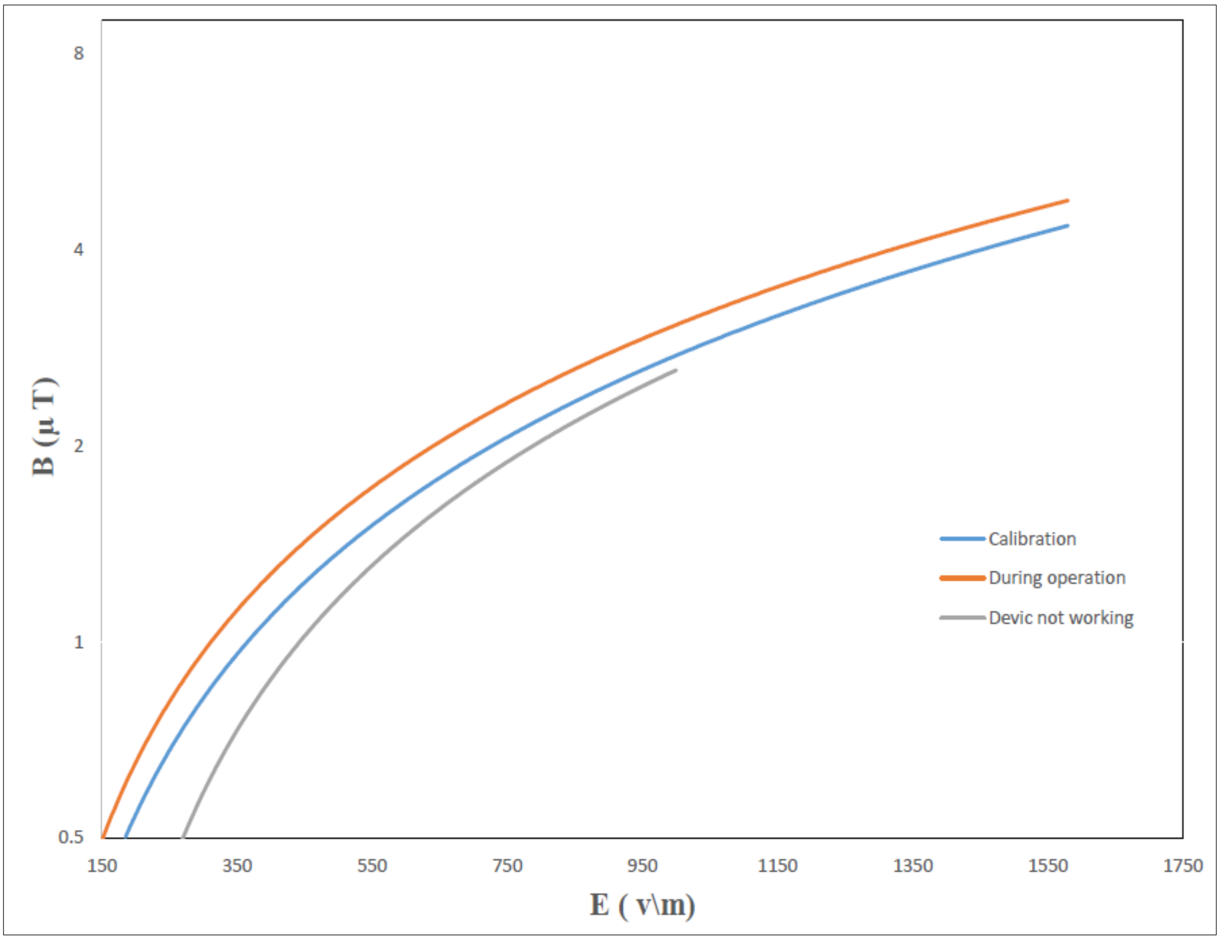

Figure 5: The relation between the electric and magnetic components in the electromagnetic radiation

X-ray Imaging System: The x-ray source of the x-ray imaging system is characterized in table 7, as follows:

Table 7: x-ray tube operating conditions

x-ray tube	(tungsten)
x-ray tube current	400 mA
x-ray tube voltage	150 KV
x-ray tube capacity	300 MHU

For detailed account of the x-ray tube Compton spectrometers the reader is referred to [8-11]. A typical arrangement for x-ray imaging system involves an x-ray tube with a tungsten (W) target; soller slits collimators, solid-state digital X-ray camera, computer, digital frame grabber, data acquisition and control card, along with appropriate software. Figure6 shows schematic presentation of the x-ray imaging system.

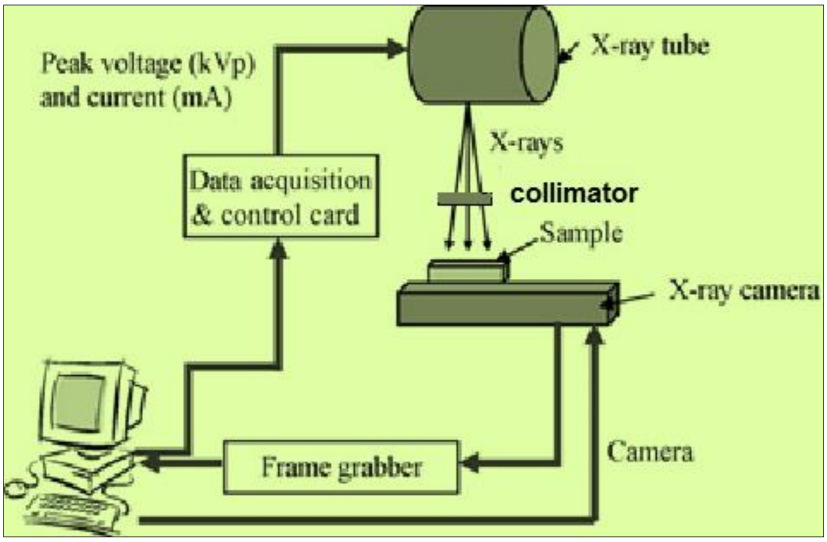

Figure 6: Schematic of X-ray imaging system [12]

Data were measured in the control room at the operator location which was at a distance of 4.20 m from the x-ray imaging system.

RESULTS AND DISCUSSION

Table 8 shows data collection at the operator position during x-ray operation.

Table 8: Measurements of electric and magnetic components of radiation emission at the operator position during x-ray operation

E(V/m)	B(T)	$\frac{1}{2}\varepsilon_0 E^2$	$\frac{1}{2\mu_0}B^2$	E_{total}	$\frac{N}{s}$
590	$2.67x10^{-6}$	$2.6119x10^{-6}$	$2.8364x10^{-6}$	$8.1724x10^{-6}$	$8.6207x10^{8}$
620	$2.85x10^{-6}$	$2.7447x10^{-6}$	$3.2318x10^{-6}$	$5.9765x10^{-6}$	$6.3043x10^{8}$
680	$2.73x10^{-6}$	$3.0104x10^{-6}$	$2.9654x10^{-6}$	$8.9637x10^{-6}$	$9.4553x10^{8}$
630	$2.20x10^{-6}$	$2.7890x10^{-6}$	$1.9257x10^{-6}$	$7.0720x10^{-6}$	$7.4599x10^{8}$
570	$1.75x10^{-6}$	$2.5234x10^{-6}$	$1.2185x10^{-6}$	$5.6128x10^{-6}$	$5.9207x10^{8}$
610	$1.25x10^{-6}$	$2.7005x10^{-6}$	$6.2169x10^{-7}$	$4.9832x10^{-6}$	$5.2566x10^{8}$
610	$0.89x10^{-6}$	$2.7005x10^{-6}$	$3.1516x10^{-7}$	$4.5234x10^{-6}$	$4.7716x10^{8}$
580	$0.93x10^{-6}$	$2.5677x10^{-6}$	$3.4413x10^{-7}$	$4.3677x10^{-6}$	$4.6073x10^{8}$
590	$0.59x10^{-6}$	$2.6119x10^{-6}$	$1.3850x10^{-7}$	$4.1256x10^{-6}$	$4.3518x10^{8}$
620	$0.59x10^{-6}$	$2.7447x10^{-6}$	$1.3850x10^{-7}$	$4.3248x10^{-6}$	$4.5620x10^{8}$
580	$0.41x10^{-6}$	$2.5677x10^{-6}$	$6.6884x10^{-8}$	$3.9518x10^{-6}$	$4.1686x10^{8}$
520	$0.23x10^{-6}$	$2.3020x10^{-6}$	$2.1048x10^{-8}$	$3.4845x10^{-6}$	$3.6757x10^{8}$
510	$0.23x10^{-6}$	$2.2578x10^{-6}$	$2.1048x10^{-8}$	$3.4182x10^{-6}$	$3.6057x10^{8}$

Figure7, summarize the results of the x-ray imaging system measurements at the operator position.

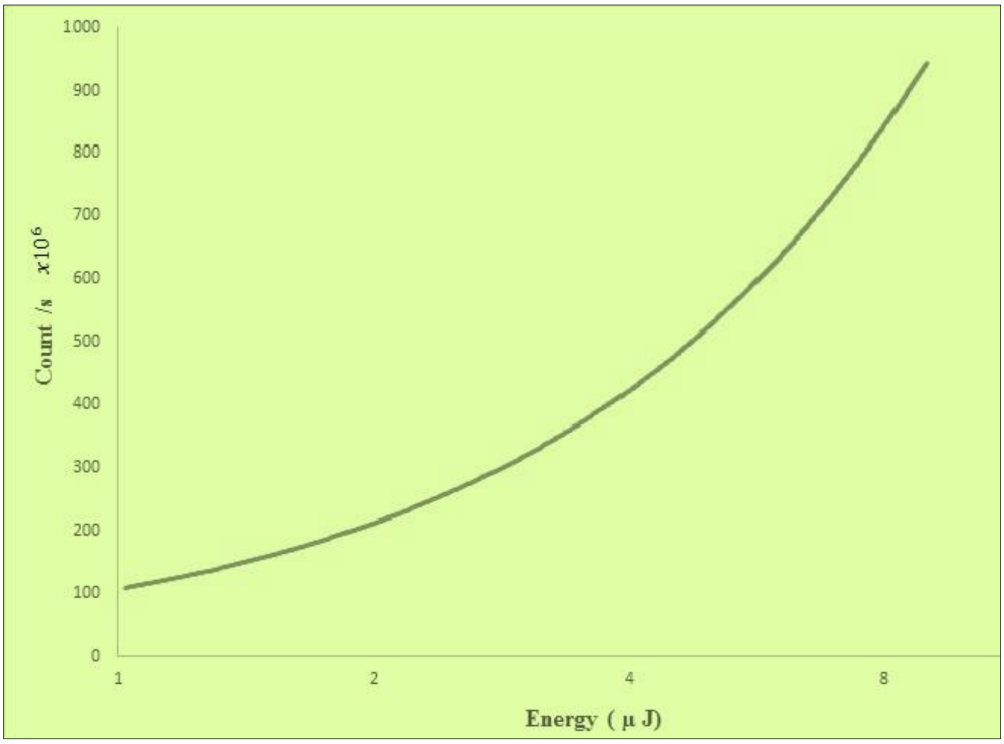

Figure 7: shows the intensity of the stray radiation with respect to kα_1 energy at the operator position

It can be seen from figure7 that there is a stray radiation from the x-ray beam directed toward the operator position. This stray radiation increases as the x-ray imaging system rotates 180 degrees.

CONCLUSION

It can be seen from the results of CT scanner and x-ray imaging system that the CT system and x-ray imaging system have bad shielding materials and this could cause severe health hazard to the operators and the personal in the control room. Therefore, a proper shielding material should be constructed and placed somewhere in the beam bath toward the operator in order to reduce this stray radiation to a large extent.

REFERENCES

1. Hamouda, S., & Amneenah, N. (2024). Electromagnetic interference impacts on electronic systems and regulations. *International Journal of Advanced Multidisciplinary Research and Studies*, *4*(1), 124-127.
2. Mangini, F., Frezza, F., Batool, S., & Bibi, A. (2019). Benefits and hazards of electromagnetic waves; telecommunication, physical and biomedical: a review. *European review for medical and pharmacological sciences*.
3. Memon, A., Godward, S., Williams, D., Siddique, I., & Al-Saleh, K. (2010). Dental x-rays and the risk of thyroid cancer: a case-control study. *Acta oncologica*, *49*(4), 447-453.
4. Shady, H., & Michael, Y. (2023). "CT-scan Image Production Procedures", StatPearls [Internet], CT-scan Image Production Procedures - StatPearls - NCBI Bookshelf (nih.gov)
5. 16.4: Energy Carried by Electromagnetic Waves - Physics LibreTexts
6. Energy in Electromagnetic Waves (utexas.edu)
7. X-ray Production, Tubes, and Generators | Radiology Key
8. Williams, B.G. (Ed.) (1977). Compton Scattering, McGraw-Hill, New York.
9. Cooper, M. J. (1977). "Compton scattering and electron momentum". *Journal Contemporary Physics*, *18*(5).
10. Cooper, M. J. (1985). Compton scattering and electron momentum determination. *Reports on Progress in Physics*, *48*(4), 415.
11. Hamouda, S. A. (2013). Gamma-ray Compton Spectroscopy for Determination of Electron Momentum Distributions in Iron. *Advanced Materials Research*, *815*, 8-12.
12. Kotwaliwale, N., Weckler, P. R., Brusewitz, G. H., Kranzler, G. A., & Maness, N. O. (2007). Non-destructive quality determination of pecans using soft X-rays. *Postharvest Biology and Technology*, *45*(3), 372-380. (PDF) Non-destructive quality determination of pecans using soft X-rays (researchgate.net)